

The impedance cardiogram recorded through two electrocardiogram/defibrillator pads as a determinant of cardiac arrest during experimental studies*

Nick Alexander Cromie, MD; John Desmond Allen, MD; Colin Turner, PhD; John McC Anderson, MPhil, DPhil; A. A. Jennifer Adgey, FACC

Objective: Laypersons are poor at emergency pulse checks (sensitivity 84%, specificity 36%). Guidelines indicate that pulse checks should not be performed. The impedance cardiogram (dZ/dt) is used to assess stroke volume. Can a novel defibrillator-based impedance cardiogram system be used to distinguish between circulatory arrest and other collapse states?

Design: Animal study.

Setting: University research laboratory.

Subjects: Twenty anesthetized, mechanically ventilated pigs, weight 50–55 kg.

Interventions: Stroke volume was altered by right ventricular pacing (160, 210, 260, and 305 beats/min). Cardiac arrest states were then induced: ventricular fibrillation (by rapid ventricular pacing) and, after successful defibrillation, pulseless electrical activity and asystole (by high-dose intravenous pentobarbitone).

Measurements and Main Results: The impedance cardiogram was recorded through electrocardiogram/defibrillator pads in standard cardiac arrest positions. Simultaneously recorded electro- and impedance cardiogram (dZ/dt) along with arterial blood pressure tracings were digitized during each pacing and cardiac

arrest protocol. Five-second epochs were analyzed for sinus rhythm (20 before ventricular fibrillation, 20 after successful defibrillation), ventricular fibrillation (40), pulseless electrical activity (20), and asystole (20), in two sets of ten pigs (ten training, ten validation). Standard impedance cardiogram variables were noncontributory in cardiac arrest, so the fast Fourier transform of dZ/dt was assessed. During ventricular pacing, the peak amplitude of fast Fourier transform of dZ/dt (between 1.5 and 4.5 Hz) correlated with stroke volume ($r^2 = .3$, $p < .001$). In cardiac arrest, a peak amplitude of fast Fourier transform of dZ/dt of ≤ 4 dB-ohm-rms indicated no output with high sensitivity (94% training set, 86% validation set) and specificity (98% training set, 90% validation set).

Conclusions: As a powerful clinical marker of circulatory collapse, the fast Fourier transformation of dZ/dt (impedance cardiogram) has the potential to improve emergency care by laypersons using automated defibrillators. (Crit Care Med 2008; 36:1578–1584)

KEY WORDS: impedance cardiography; Fourier analysis; cardiopulmonary resuscitation; pulse check

Pulse checks by laypersons delay resuscitation and are poor indicators of cardiac arrest (sensitivity 84%, specificity 36%), causing an average delay of 24 secs (1–3).

The current International Liaison Committee on Resuscitation/Emergency Cardiovascular Care guidelines dictate that laypersons should not check for a pulse during assessment of collapsed patients (1, 2, 4, 5).

Emergency Cardiovascular Care training programs and public access defibrillator schemes (6–8) have provided laypersons who are skilled in applying transthoracic electrodes and using automated external defibrillators (AEDs). How can automated defibrillator systems recognize circulatory arrest in addition to diagnosing cardiac rhythm? A hemodynamic sensor automatically diagnosing cardiac arrest, together with current electrocardiogram (ECG) algorithms, would aid in the management of collapsed patients, for whom critical decisions must be made. ECG algorithms are unable to distinguish pulse-

less electrical activity (PEA) from sinus rhythm. In ventricular tachycardia, hemodynamic disturbance dictates immediate defibrillation.

Recent improvements in recording methods have led to widespread use of impedance cardiography (ICG; dZ/dt) in critical care (9, 10). However, four-electrode systems are impracticable in cases of out-of-hospital cardiac arrest (11, 12).

The objective of this laboratory study was to develop and assess a simplified ICG system by recording from two transthoracic ECG/defibrillation pads during experimental cardiac arrest.

MATERIALS AND METHODS

Changes in the transthoracic impedance are related mainly to variations in arterial and not cardiac blood volume (13). The theoretical basis for the standard method of ICG recording was developed by Kubicek et al. (14, 15),

*See also p. 1677.

From Regional Medical Cardiology Centre, Royal Victoria Hospital, Belfast (NAC, AAJA); Physiology, Queen's University Belfast (JDA); School of Electrical and Mechanical Engineering, University of Ulster (CT); and NI BioEngineering Centre, University of Ulster, Northern Ireland (JMA).

Dr. Anderson is senior vice-president (science and engineering), Heartsine Technologies, Ltd. Dr. Cromie was sponsored by Research and Development Office, DHSSPS Northern Ireland, UK. The remaining authors have not disclosed any potential conflicts of interest.

Address requests for reprints to: Nick Cromie, MD, Regional Medical Cardiology Centre, Royal Victoria Hospital, Belfast, Northern Ireland, BT12 6BA. E-mail: nacromie@doctors.org.uk

Copyright © 2008 by the Society of Critical Care Medicine and Lippincott Williams & Wilkins

DOI: 10.1097/CCM.0b013e318170a03b

where stroke volume (SV) is estimated as follows (15, 16):

$$SV_{\text{impedance}} = \rho_b \cdot (L^2/Zo^2) \cdot T \cdot dZ/dt_{\text{max}} \quad [1]$$

where ρ_b is blood resistivity ($\Omega\text{-cm}$), L the distance between the two voltage-sensing electrodes (cm), Zo the mean steady-state basal impedance (Ω), dZ/dt_{max} the peak negative deflection of dZ/dt waveform (proportional to peak ascending aortic flow (Ωs^{-1}) (17, 18), and T the left ventricular ejection time (seconds).

The standard ICG requires at least four electrodes (two for voltage recording, two for current application) to determine changing transthoracic impedance (14, 15). Recording the ICG through two defibrillation pads may have limitations. Since only a vector of total transthoracic impedance is recorded, the computed ICG signal may be less specific. Baseline transthoracic impedance and left ventricular ejection time are not obtainable in cardiac arrest.

An experimental defibrillator was constructed (Samaritan AED, HeartSine Technologies, UK) to determine ICG from a low-amplitude sinusoidal current (30 kHz, 0.05 mA) between the two defibrillator pads (11) and defibrillate (CE-mark standard). Adhesive defibrillator pads (Samaritan, SDE 201) in standard cardiac arrest positions (inferior to right clavicle in midclavicular line, to right of upper sternum, and over left lower chest) monitored ECG and ICG. The ECG, ICG, and defibrillator shocks were digitized and stored for later analysis.

General Methods. Pigs (Landrace–Large White cross, weight 50–55 kg, mean $sd \pm 52.5$ 1.8 kg, eight male, 12 female) were fasted and sedated with intramuscular azaperone (1 mg/kg; Janssen Pharmaceuticals, Beerse, Belgium). Anesthesia was induced (pentobarbitone sodium 20–24 mg/kg intravenously) and maintained by intravenous infusion (360–720 mg/hr). Endotracheal ventilation (room air, adjusted tidal volume) maintained normal end-tidal CO_2 and tissue oxygen saturation (Datex-Ohmeda, GE Healthcare, Giles, UK). Body temperature was checked with a rectal probe and homeothermic control unit (Harvard Instruments, Holliston, MA).

The external jugular veins and carotid artery were cannulated. Carotid arterial blood pressure was monitored by transducer (Druck, New Fairfield, CT). A ventricular pacing catheter (Cordis 103998, Miami, FL) was placed in the right ventricular apex under radiographic control (Siemens Siremobil 3H, Berkshire, UK). Cardiac output was determined by thermodilution (three recordings averaged, injectate 10 mL of 5% dextrose, $<4^\circ\text{C}$, Baxter-Edwards COM-1, Valencia, CA), with pulmonary artery flotation catheter in the pulmonary artery.

The ECG, ICG (Z/t , which is the change in total impedance over time before the first order derivative dZ/dt is calculated), arterial blood

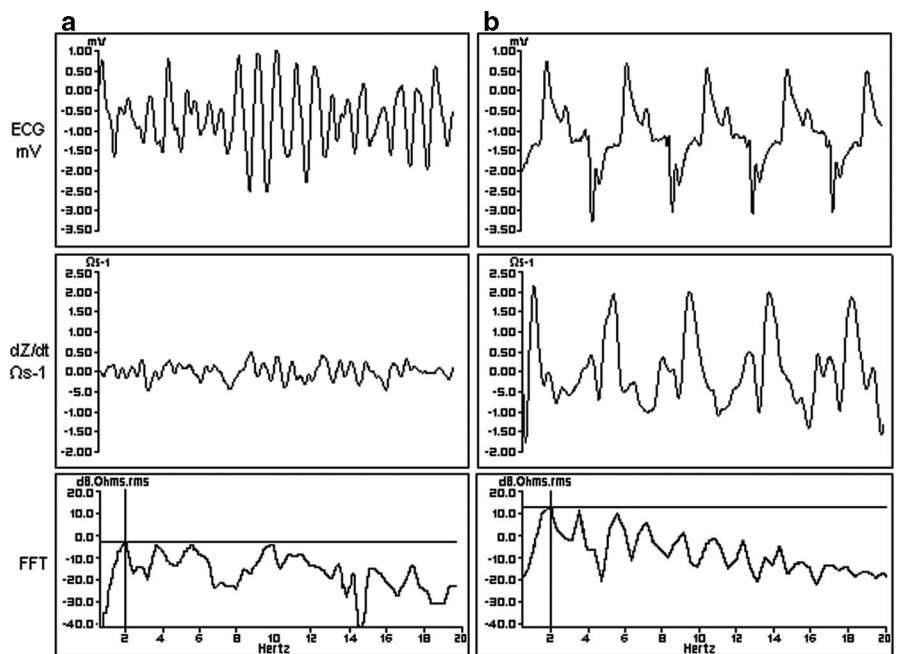


Figure 1. A 2.5-sec record showing the electrocardiogram (ECG, top), the dZ/dt impedance cardiogram (middle), and the fast Fourier transformation (FFT) of dZ/dt (bottom), recorded through two electrocardiogram/defibrillation pads, during experimental ventricular fibrillation (a) and after successful defibrillation (b) in the same animal. Note that although the signals in both a and b are oscillatory, during sinus rhythm (b) the impedance cardiography signal amplitude is greater, and the frequency is more regular with a resultant larger peak of the FFT between 1.5 and 4.5 Hz. In sinus rhythm, the peak amplitude of the FFT of dZ/dt (between 1.5 and 4.5 Hz) is found at 2.0 Hz (12.59 dB-ohm-rms). This is consistent with a heart rate of 120 beats/min.

pressure, and pacing waveforms (Grass S88 stimulator, Grass Technologies, Rockland, MA) were recorded on laboratory computer (digitization 1 kHz; BioBench, National Instruments, Berkshire, UK). The first-order derivative of the ICG (dZ/dt) was obtained retrospectively (BioBench; Fig. 1). Channels were calibrated daily. Pigs lay supine, and thoracic hair was clipped. Ventilation was stopped during recordings. Experimental procedures adhered to the Animals (Scientific Procedures) Act, 1986 (UK), and were approved by the University Experimental Ethical Review Committee.

Two different protocols were followed: protocol 1—pacing studies and protocol 2—cardiac arrest studies.

Protocol 1—Pacing Studies. In 20 pigs, the right ventricle was paced at a rate of 160 beats/min at the threshold voltage, and stroke volume was determined. After ventilation was stopped, the ECG, ICG, arterial blood pressure, and pacing activity were recorded simultaneously (pacing 160 at threshold).

This protocol was duplicated for 210 beats/min (pacing 210 at threshold), 260 beats/min (pacing 260 at threshold), and 305 beats/min (pacing 305 at threshold). Data from 5-sec periods of uninterrupted pacing were analyzed retrospectively at each pacing rate and stimulation voltage ($\times 2$ threshold, data not shown).

Stroke volumes by thermodilution and ICG-derived variables should show similar changes at varied paced heart rates. Nonpara-

metric correlation coefficients (Spearman's) were determined between stroke volume by thermodilution and the following variables:

dZ/dt_{max} ; dZ/dt_{max} corrected for baseline impedance obtained between the two ECG/defibrillator pads, that is, $(dZ/dt_{\text{max}})/Zo^2$ (from Eq. 1); and peak amplitude of the dZ/dt frequency spectrum between 1.5 and 4.5 Hz, by fast Fourier transformation (FFT; BioBench, Fig. 1).

Statistical significance of differences was assessed in both protocols (SPSS 12.0.1 for Windows, SPSS, Chicago, IL; $p < .05$ as the level for significance).

Protocol 2—Cardiac Arrest Studies. Two groups, each with ten pigs, were studied. The first group was used to develop the algorithm (the training set), the second group to validate the algorithm (the validation set). Cardiac output by thermodilution, with ECG, ICG, and arterial blood pressure, was obtained at baseline before initiation of this experimental protocol in each group.

Two sequential episodes of ventricular fibrillation (VF; Fig. 1a), PEA, and asystole were induced in each group of ten pigs. Rapid right ventricular pacing induced VF. For each brief episode of VF, four 5-sec recordings were taken: sinus rhythm before induction (sinus rhythm, SR1), during VF (at 2–7 and 7–12 secs after induction, VF1, VF2), and finally at

10–15 secs after successful defibrillation (SRr; Fig. 1b). After successful defibrillation, the systolic blood pressure was always >70 mm Hg during sinus rhythm. Two episodes of VF were induced in each animal. From the first episode recordings 1SR1, 1VF1, 1VF2, and 1SRr were obtained and from the second episode recordings 2SR1, 2VF1, 2VF2, and 2SRr.

PEA was induced by a large bolus of pentobarbitone sodium (4 g intravenously; Fig. 2). Recordings were made at 10–15 and 60–65 secs after induction of PEA (PEA1 and PEA2, respectively) and during subsequent electrical asystole, when intrinsic cardiac electrical activity had ceased for 30–35 and 45–50 secs (asystole 1 and asystole 2, respectively).

For each pig in the training and validation sets (ten pigs/set), there were two recordings during sinus rhythm at baseline (SR1) and after successful defibrillation (SRr), four during VF, two during PEA, and two during asystole.

From equation 1, ICG stroke volume is proportional to dZ/dt_{\max} , the maximum negative deflection of the first-order derivative (Ωs^{-1}). For each 5-sec epoch, dZ/dt_{\max} was determined (digital filter bandwidth of 1–11 Hz), and the FFT frequency spectrum of the dZ/dt waveform was examined for its peak amplitude between 1.5 and 4.5 Hz (dB·ohm·rms; BioBench, National Instruments, Austin, TX; Fig. 1).

Results are reported as mean \pm sd, with interquartile ranges and 95% confidence intervals where appropriate. The statistical significance of differences was assessed (SPSS 12.0.1 for Windows). Sensitivities and specificities were calculated to distinguish sinus from cardiac arrest states.

The authors had full access to the data and take responsibility for its integrity. All authors read and approved this report.

RESULTS

Protocol 1—Pacing Studies. The basic hemodynamic and other variables in the 20 pigs are shown (Table 1). During sinus

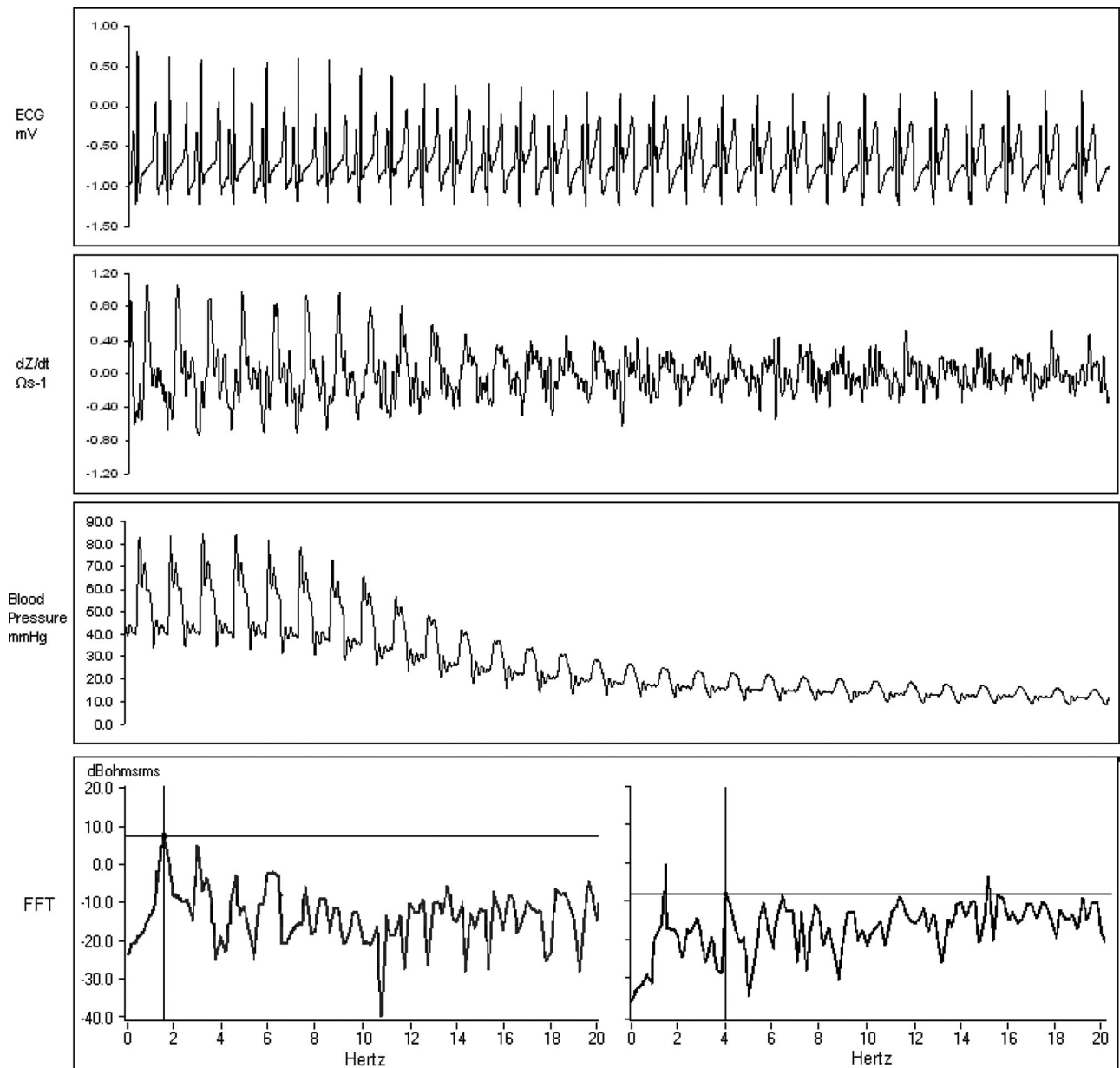


Figure 2. A 20-sec record of the electrocardiogram (ECG, top), impedance cardiography (ICG) (dZ/dt , second down), and arterial blood pressure tracing (third down) at the onset of pharmacologically induced pulseless electrical activity. As the blood pressure decreases, the ICG signal amplitude and the peak fast Fourier transformation (FFT) between 1.5 and 4.5 Hz (bottom, peak signal marked) also decrease. The ECG and heart rate remain relatively unchanged.

Table 1. Cardiovascular parameters during sinus rhythm in training and validation sets

	All (Pacing + Cardiac Arrest)	Training (Cardiac Arrest)	Validation (Cardiac Arrest)
Number of pigs	20 (8 male)	10 (4 male)	10 (4 male)
Body weight (kg)	52.5 ± 1.77	52.6 ± 1.7	52.9 ± 1.9
Heart rate during sinus rhythm (beats/min)	117 ± 19	114 ± 25	120 ± 10
Cardiac output (L/min)	6.38 ± 1.16	5.95 ± 1.1	6.81 ± 1.1
Systolic BP (mm Hg)	111 ± 25	120 ± 27	102 ± 20
Diastolic BP (mm Hg)	81 ± 25	85 ± 30	77 ± 21

BP, blood pressure.

Data are shown as mean ± SD. No significant differences were observed between the groups.

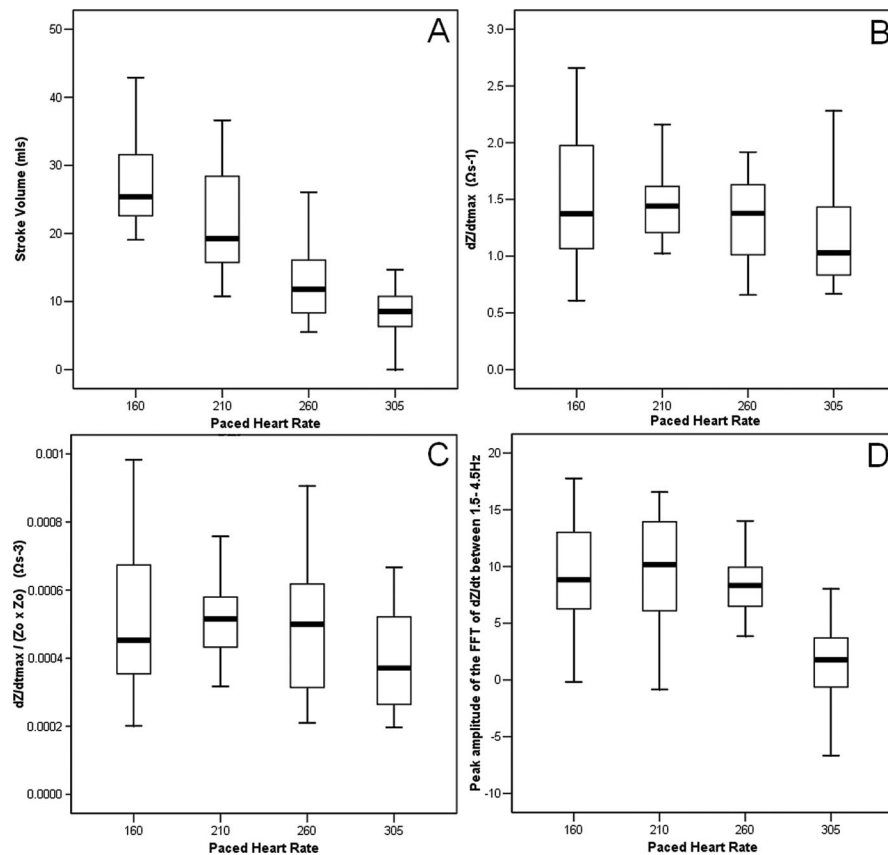


Figure 3. Box plots showing medians and interquartile ranges for stroke volumes (A), dZ/dt_{max} (B), $(dZ/dt_{max})/Zo^2$ (C), and the peak amplitude of the fast Fourier transformation (FFT) of dZ/dt between 1.5 and 4.5 Hz (D), in 20 pigs with pacing at 160, 210, 260, and 305 beats/min. There is a progressive decrease in stroke volume over the pacing range (A), with a sudden decrease in peak amplitude of the FFT of dZ/dt (D) between pacing at 260 and pacing at 305 beats/min. dZ/dt_{max} , peak negative deflection of dZ/dt waveform; Zo , mean steady-state basal impedance.

rhythm, the ECG and ICG records showed similar rhythmic oscillations; the FFT of dZ/dt peaked between 1.5 and 4.5 Hz, with harmonics (Fig. 1b).

The effects of right ventricular cardiac pacing on stroke volume and the ICG signal were determined at 160, 210, 260, and 305 beats/min in 20 pigs. From 80 potential results, three data values from three experiments were excluded in the subsequent analysis, leaving 77 data points. In two experiments, pacing at 305

beats/min caused problems (one VF, one failure to capture). In one experiment, pacing at 160 beats/min failed (baseline heart rate 190 beats/min).

Stroke volume decreased progressively as pacing rate increased (Fig. 3A). The peak amplitude of the FFT of dZ/dt (between 1.5 and 4.5 Hz) remained fairly consistent until a sudden decrease on pacing at 305 beats/min (Fig. 3D). Median stroke volume of 11.82 mL (interquartile range 8.07–16.49 mL) at pacing at 260 beats/min fell to 8.57

mL (interquartile range 6.23–11.15) during pacing at 305 beats/min (Fig. 3).

By equation 1, dZ/dt_{max} and $(dZ/dt_{max})/Zo^2$ are directly related to stroke volume. However, relatively poor linear correlations were obtained between stroke volume and either dZ/dt_{max} ($r^2 = .07, p = .02$) or $(dZ/dt_{max})/Zo^2$ ($r^2 = .06, p < .05$; Table 2). These traditional ICG variables (Eq. 1) showed poor correlations with stroke volume when recorded through two ECG/defibrillation pads (Table 2).

Stroke volume correlated better with the peak amplitude of the FFT of dZ/dt between 1.5 and 4.5 Hz ($r^2 = .30, p < .001$; Table 2), supporting the use of this variable as a hemodynamic marker.

Protocol 2—Cardiac Arrest Studies. The data obtained from the first and second episodes of ventricular fibrillation (1VF1, 1VF2, 2VF1, 2VF2; Fig. 1a) were compared with those during sinus rhythm in the same animals, both before (1SR1, 2SR1) and after defibrillation (1SRr, 2SRr; Fig. 1b). During sinus rhythm, baseline hemodynamic and other variables showed no significant differences between the training and validation sets (Table 1).

With the onset of VF, there was a dramatic decrease in the maximum amplitude of FFT of the dZ/dt waveform between 1.5 and 4.5 Hz. The change in peak amplitude of dZ/dt_{max} was less marked, especially for the first episode of VF (1VF1, 1VF2; Table 3).

The data obtained during PEA (Fig. 2) and cardiac asystole confirmed the results seen during VF (Table 3 and Fig. 4). The decrease in peak amplitude of the FFT of dZ/dt (between 1.5 and 4.5Hz) during PEA and asystole was significantly different from the values during sinus rhythm, both before VF (1SR1 + 2SR1) and after (1SRr + 2SRr) recovery from defibrillation ($p < .001$; Table 3). Again, changes in peak dZ/dt_{max} were less marked ($p < .05$) during both PEA and asystole.

For the training set data, a peak amplitude of the FFT of $dZ/dt \leq 4$ dB-ohm-rms gave good sensitivity as an indicator of cardiac arrest without adversely affecting specificity. When compared with the ECG and arterial blood pressure, this dZ/dt FFT amplitude predicted the presence of cardiac arrest with a sensitivity of $94\% \pm 4.2\%$ and specificity of $98\% \pm 2.5\%$ ($\pm 95\%$ confidence interval). The same dZ/dt FFT criterion was then applied to the validation set. FFT amplitude (≤ 4 dB-ohm-rms) indicated

Table 2. Correlation coefficients for the ICG parameters with stroke volume by thermodilution, altered by a pacing protocol (n = 77)

	Correlation with Stroke Volume (r)	Correlation with Stroke Volume (r ²)	Significance (2-tailed)
dZ/dt _{max} (Ωs ⁻¹)	.268	.072	.018
(dZ/dt _{max})/Zo ² (Ωs ⁻³)	.242	.059	.034
Peak amplitude of the FFT of dZ/dt between 1.5–4.5 Hz (dB.ohms.rms)	.547	.299	<.001

dZ/dt_{max}, peak negative deflection of dZ/dt waveform; FFT, fast Fourier transformation; ICG, impedance cardiography; Zo, mean steady-state basal impedance.

Table 3. dZ/dt_{max} (Ωs⁻¹) and peak amplitude of the FFT of dZ/dt between 1.5–4.5Hz (dB.ohms.rms) are shown for 20 pigs (mean ± SD)

Rhythm	Mean Peak dZ/dt _{max} (Ωs ⁻¹)	Mean Peak FFT Amplitude @ 1.5–4.5 Hz (dB.ohms.rms)
Episode 1SR1	1.25 ± .69	7.02 ± 2.75
1VF1	1.30 ± 1.17	.14 ± 3.63 ^c
1VF2	1.04 ± .80 ^b	-.12 ± 3.62 ^c
Recovery 1SRr	2.10 ± .68	8.56 ± 3.64
Episode 2SR1	1.65 ± .43	8.53 ± 3.79
2VF1	1.00 ± .57 ^c	.16 ± 3.92 ^c
2VF2	1.05 ± .49 ^c	.36 ± 4.8 ^c
Recovery 2SRr	2.10 ± .88	9.5 ± 2.92
PEA1	1.00 ± .87 ^a	-1.72 ± 4.41 ^d
PEA2	.98 ± .95 ^a	-6.28 ± 4.68 ^d
Asystole1	.91 ± .87 ^a	-8.98 ± 6.47 ^d
Asystole 2	.96 ± 1.07 ^a	-9.50 ± 6.95 ^d

dZ/dt_{max}, peak negative deflection of dZ/dt waveform; FFT, fast Fourier transformation.

Values are shown during sinus rhythm (SR) and in 3 circulatory arrest states. Two sequential episodes of ventricular fibrillation (VF), pulseless electrical activity (PEA) and asystole were induced. For each brief episode of VF, 4 5-second epochs were recorded: one prior to induction (sinus rhythm; SR1), two during VF (VF1, VF2), and the final after successful defibrillation (SRr). From the first VF episode 1SR1, 1VF1, 1VF2, and 1SRr were obtained, and from the second 2SR1, 2VF1, 2VF2, and 2SRr. Two epochs were then recorded following induction of PEA (PEA1 and PEA2) and 2 during asystole (asystole 1 and asystole 2).

^aindicates significant differences for PEA and asystole (*p* < .05) with each epoch of sinus rhythm (1SR1, 2SR1, 1SRr, and 2SRr). ^band ^cindicate a significant difference (*p* < .01 and *p* ≤ .001, respectively) for that VF epoch and sinus rhythm both before (SR1) and after its successful defibrillation (SRr). ^dindicates significant differences for PEA and asystole (*p* < .001) with each epoch of sinus rhythm (1SR1, 2SR1, 1SRr, and 2SRr).

cardiac arrest with sensitivity 86% ± 6.2% and specificity 90% ± 5.4% vs. ECG and arterial blood pressure (5-sec epochs).

Failure in sensitivity for the algorithm occurred in the training set in four of 40 examples of VF and only one of 20 cases of PEA. In the validation set, failure occurred in eight (of 40) examples of VF, two (of 20) cases of PEA, and one (of 20) cases of asystole. The two PEA failures and one asystole failure occurred in the same animal, a 50-kg female swine; diagnostic values (peak FFT ≤ 4 dB-ohm-rms) were seen in the preceding 5-sec epochs of PEA but not in asystole. This suggests that some variability in the FFT may be seen during sustained PEA.

DISCUSSION

Correct and uncomplicated advice for first responders during management of the collapsed patient is crucial. How can syncopal patients with cardiac output be differentiated from patients in cardiac arrest, for example, due to a PEA rhythm? Can automated defibrillator algorithms distinguish a patient with pulseless VT from nonpulseless VT? An automated check (hemodynamic sensor) of circulatory status could aid in the management of such patients without requiring additional training for laypersons. The traditional ICG variables of left ventricular ejection time and baseline impedance

(14–16, 18) are not available in cardiac arrest. During cardiac arrest, the role of the ICG is to indicate presence or absence of cardiac output. This has been achieved in the present experiments by signal analysis methods (FFT).

The present results show that over an assessment period of 5 secs, impedance cardiography is a powerful hemodynamic sensor of cardiac arrest, when the peak amplitude of the FFT of the dZ/dt is ≤ 4 dB-ohm-rms. The high sensitivities (94% ± 4.2% training set; 86% ± 6.2% validation set) and high specificities (98% ± 2.5% training set; 90% ± 5.4% validation set) exceed those for detection of an absent pulse by laypersons (84% sensitivity, 36% specificity), which also caused delay with a mean time to decision of 24 secs (3). In this experimental model, dZ/dt_{max} was not as effective in determining cardiac arrest as peak amplitude of FFT of dZ/dt.

Stroke volume during right ventricular pacing showed poor correlations with dZ/dt_{max}, even when corrected for baseline impedance ([dZ/dt_{max}]/Zo²). Stroke volume correlated better with the peak amplitude of the FFT of dZ/dt between 1.5 and 4.5Hz. While a signal-averaged ICG dZ/dt_{max} may correlate better with stroke volume during sinus rhythm (12, 19), a signal-averaged ICG cannot contribute to the diagnosis of asystole or VF, the major causes of cardiac arrest. In the present experiments, the peak amplitude of the FFT of dZ/dt successfully distinguished cardiac arrest states from sinus rhythm.

Although differences in sensitivity and specificity were noted between training and validation sets, 95% confidence intervals overlapped considerably for sensitivity and were close for specificity. Diagnostic failure in the validation set arose from failed assessment of VF. Records were obtained soon after VF onset, all within the first 12 secs of onset, when some degree of oscillatory flow may remain. If so, would recording of later VF result in less algorithm failure? Current AED ECG algorithms have sensitivity approaching 100% for detection of VF, so an ICG algorithm would give little benefit for VF diagnosis. An ECG algorithm alone was reported to distinguish PEA with high sensitivity (90%) from a pulse-circulating rhythm (specificity 85%) in 191 three-second epochs from 653 cardiac arrests (20). However, it is not clear how physician teams decided which ECG

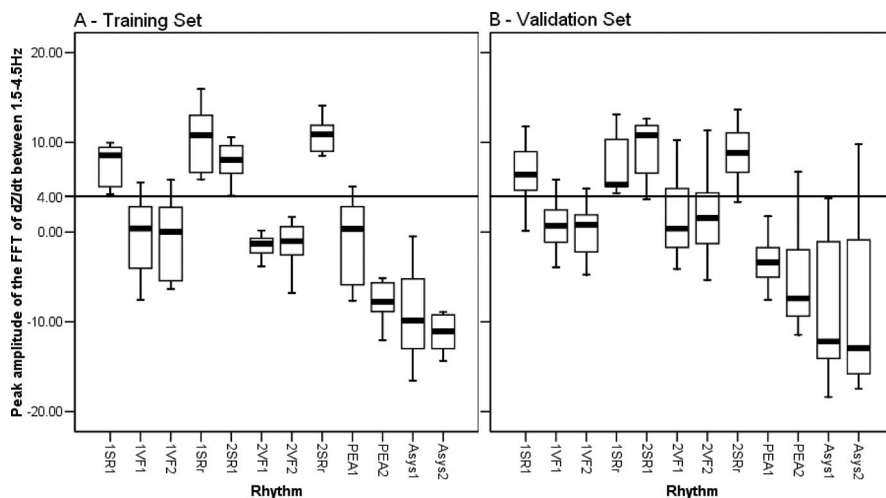


Figure 4. Box plots showing medians and interquartile ranges (IQRs) for the peak amplitude of the fast Fourier transformation (FFT) of dZ/dt recorded pre- and postarrest and during each of the cardiac arrest states for both training (A) and validation sets (B). For all cardiac arrest states, there was no overlap of IQRs with those for sinus rhythm. The algorithm cutoff value of 4 dB-ohm-rms is also shown as a horizontal line. *ISRI* and *2SR1*, sinus rhythm before induction, first and second episodes, respectively; *1VF1* and *1VF2*, sinus rhythm during ventricular fibrillation (at 2–7 and 7–12 secs after induction, respectively), first episode; *2VF1* and *2VF2*, sinus rhythm during ventricular fibrillation (at 2–7 and 7–12 secs after induction, respectively), second episode; *1SRr* and *2SRr*, sinus rhythm 10–15 secs after successful defibrillation, first and second episodes, respectively; *PEA1* and *PEA2*, 10–15 and 60–65 secs after induction of pulseless electrical activity, respectively; *Asys1* and *Asys2*, during subsequent electrical asystole, when intrinsic cardiac electrical activity had ceased for 30–35 and 45–50 secs, respectively.

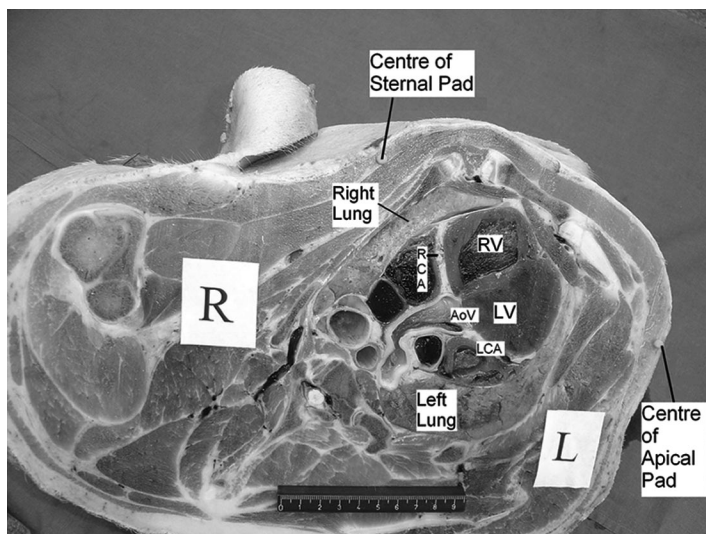


Figure 5. Porcine thoracic transection, showing the center of the apical and sternal defibrillation/electrocardiograph pads, the left and right lung, the left and right ventricle (LV and RV), the left and right coronary arteries (LCA and RCA), and the aortic valve (AoV).

tracings were PEA and which patients had a circulating pulse.

In the present studies, the ICG was recorded during episodes of experimental apnea. In clinical use during agonal breathing or ventilation, the peak amplitude of FFT of dZ/dt should separate cardiac output signals from respiratory artifact. Both respiratory activity and cardiac activity cause fluctuations in transtho-

rac impedance but at different frequencies, so the spectra can be easily differentiated (21).

Major fluctuations in the ICG relate to peak aortic flow (17, 18), and we have analyzed the frequency spectrum. Can these methods be transposed to the human subject? The porcine heart and thorax show similarities to human anatomy (Fig. 5). Pigs and humans show compa-

able fluctuations in frequency and magnitude of transthoracic ICG tracings, recorded through two ECG/defibrillator pads.

Many AEDs are equipped with an impedance channel, so this system would be easily applicable to clinical practice and could be readily implemented. Automated defibrillators with dynamic ICG detection, in addition to current ECG algorithms, can potentially advise bystanders to commence cardiopulmonary resuscitation in VF, VT, PEA, and asystolic arrests. Importantly, such devices could also monitor patients during postresuscitation care (Fig. 1). Automated signal analysis by this simple system would inform defibrillator users of circulatory status.

CONCLUSION

The frequency spectrum of the impedance cardiogram recorded through two transthoracic defibrillator pads is a marker of circulatory collapse. These studies support use of ICG signals in defibrillator design and emergency care.

ACKNOWLEDGMENTS

We thank Allister McIntyre, PhD, Jim Allen, PhD, and Ms Rebecca DiMaio of Heartsine Technologies, Belfast, for engineering support. Dr Cromie was sponsored by Research and Development Office, DHSSPS-NI, UK.

REFERENCES

- Cummins RO, Hazinski MF: The most important changes in the international ECC and CPR guidelines 2000. *Circulation* 2000; 102:I-371-I-376
- Cummins RO, Hazinski MF: Guidelines based on fear of type II (false-negative) errors: Why we dropped the pulse check for lay rescuers. *Circulation* 2000; 102:I-377-I-379
- Eberle B, Dick WF, Schneider T, et al: Checking the carotid pulse check: Diagnostic accuracy of first responders in patients with and without a pulse. *Resuscitation* 1996; 33: 107–116
- Guidelines 2000 for Cardiopulmonary Resuscitation and Emergency Cardiovascular Care: Part 3. Adult basic life support. The American Heart Association in collaboration with the International Liaison Committee on Resuscitation. *Circulation* 2000; 102(Suppl): I22–I59
- Handley AJ, Becker LB, Allen M, et al: Single-rescuer adult basic life support: An advisory statement from the Basic Life Support Working Group of the International Liaison Committee on Resuscitation (ILCOR). *Circulation* 1997; 95:2174–2179

6. Capucci A, Aschieri D, Piepoli MF, et al: Tripling survival from sudden cardiac arrest via early defibrillation without traditional education in cardiopulmonary resuscitation. *Circulation* 2002; 106:1065–1070
7. Culley LL, Rea TD, Murray JA, et al: Public access defibrillation in out-of-hospital cardiac arrest: A community-based study. *Circulation* 2004; 109:1859–1863
8. van Alem AP, Vrenken RH, de Vos R, et al: Use of automated external defibrillator by first responders in out of hospital cardiac arrest: Prospective controlled trial. *BMJ* 2003; 327:1312–1315
9. Packer M, Abraham WT, Mehra MR, et al; for the Prospective Evaluation and Identification of Cardiac Decompensation by ICG Test (PREDICT) Study Investigators and Coordinators: Utility of impedance cardiography for the identification of short-term risk of clinical decompensation in stable patients with chronic heart failure. *J Am Coll Cardiol* 2006; 47:2245–2252
10. Mehra MR: Optimizing outcomes in the patient with acute decompensated heart failure. *Am Heart J* 2006; 151:571–579
11. Johnston PW, Imam Z, Dempsey G et al: The transthoracic impedance cardiogram is a potential haemodynamic sensor for an automated external defibrillator. *Eur Heart J* 1998; 19:1879–1888
12. Losert H, Risdal M, Sterz F et al: Thoracic-impedance changes measured via defibrillator pads can monitor signs of circulation. *Resuscitation* 2007; 73:221–228
13. Bonjer FH, Van Den Berg JW, Dirken MNJ: The origin of the variations of body impedance occurring during the cardiac cycle. *Circulation* 1952; 6:415–420
14. Kubicek WG, Karnegis JN, Patterson RP, et al: Development and evaluation of an impedance cardiac output system. *Aerosp Med* 1966; 37:1208–1212
15. Kubicek WG, Kottke J, Ramos MU, et al: The Minnesota impedance cardiograph- theory and applications. *Biomed Eng* 1974; 9:410–416
16. Bernstein DP: A new stroke volume equation for thoracic electrical bioimpedance: Theory and rationale. *Crit Care Med* 1986; 14: 904–909
17. Kubicek WG: On the source of peak first time derivative (dZ/dt) during impedance cardiography. *Ann Biomed Eng* 1989; 17:459–462
18. Woltjer HH, Bogaard HJ, de Vries PMJM: The technique of impedance cardiography. *Eur Heart J* 1997; 18:1396–1403
19. Miyamoto Y, Takahashi M, Tamura T, et al: Continuous determination of cardiac output during exercise by the use of impedance plethysmography. *Med Biol Eng Comput* 1981; 19:638–644
20. Risdal M, Steen PA, Kramer-Johansen J, et al: Discriminating between PEA and pulse circulating rhythm using ECG. *Resuscitation* 2006; 69:46
21. Losert H, Risdal M, Sterz F et al: Thoracic impedance changes measured via defibrillator pads can monitor ventilation in critically ill patients and during cardiopulmonary resuscitation. *Crit Care Med* 2006; 34: 2399–2405